Welding in the World (2019) 63:1561–1572
https://doi.org/10.1007/s40194-019-00779-0

RESEARCH PAPER

Improvement of the joint quality in the high-frequency induction welding of pipes by edge modification

Morteza Ghaffarpour[1] · Davood Akbari[1] · Hasan Moslemi Naeeni[1] · Sajad Ghanbari[1]

Received: 21 January 2019 / Accepted: 12 July 2019 / Published online: 30 July 2019
© International Institute of Welding 2019

Abstract

High-frequency induction welding (HFIW) is among the most commonly used methods for producing roll formed pipes. In this paper, weld quality is evaluated through examining the weld properties, in order to obtain the effect of edge preparation on improvement of weld quality. Temperature distribution in the weld zone is studied through the groove shape of the weld joint, and the other parameters such as current, frequency, and linear speed, considered constant, are equal to 1400 A, 150 kHz, and 25 m/min respectively. The mechanical and metallurgical properties of the weld metal were evaluated by tensile test and metallography. The appropriate temperature distribution resulted from modifying the shape of the connecting edges, leading to a reduction of 27% in the mean size of the grains in the weld zone. The results also show that by increasing the temperature of welding, the heat-affected area expands and the other areas decrease. When the results of the metallography tests of the weld zone were compared, a more uniform weld width was observed in the welded specimens with modified edges. The results also showed an 18% decrease in the weld width in specimens, compared with the specimens without edge preparation.

Keywords High-frequency induction welding (HFIW) · Magnetic-thermal analysis · Joint edge shape · Temperature gradient

1 Introduction

High-frequency induction welding (HFIW) is the most frequent process of welding welded pipes. Thus, the quality of this process directly affects the quality of the final products. The HFIW process takes place in the ending station of the roll forming process to connect the edges of the closed profiles. So, it has a critical effect on the quality of the final profiles produced. The HFIW process is widely used in pipe and profiles industry, as it is a high-speed, automatic, and continuous manufacturing method. As shown in Fig. 1, a high-frequency induction coil is used as an inductor to connect the edges of the pipe by means of the high-frequency electrical current. HFIW process takes place as a continuous process. In this process, the electric flux vortex flows in the pipe surface and the edges undergo an extremely high temperature due to the high-frequency electric flux.

Since the welded pipes are widely used in the oil and gas industry, and due to the need for a high reliability, induction weld quality should improve. Also, as this process is continuous, improper parameters reduce the weld quality, imposing heavy costs. One of the most important parameters affecting the quality of the welded joint is the geometry of the beveled edge. According to the initial edge geometry of the sheet, a different edge angle will appear in the final station of the role-formed sheet, which differs in the outer and inner parts of the joint. It is evident in the sheets of 5 mm of thickness and more that the edge preparation affects the quality of the welded joint [1]. Since high-schedule pipes are widely used in high working pressures, the quality of the seam-welded edges is very important.

✉ Davood Akbari
daakbari@modares.ac.ir

Morteza Ghaffarpour
m.ghaffarpour@modares.ac.ir

Hasan Moslemi Naeeni
moslemi@modares.ac.ir

Sajad Ghanbari
s.ghanbari@modares.ac.ir

[1] Department of Mechanical Engineering, Tarbiat Modares University, Tehran, Iran

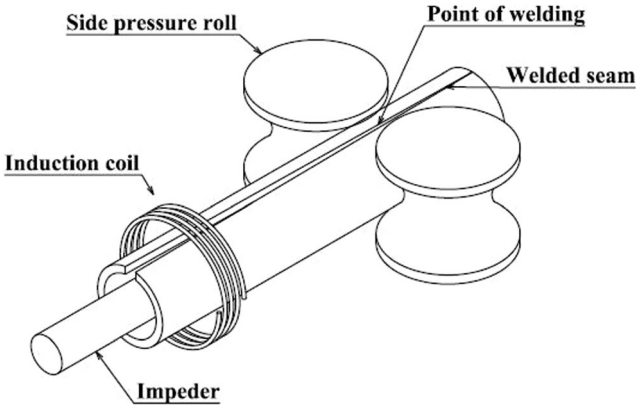

Fig. 1 Schematic of high-frequency induction welding process

In recent years, many studies were conducted on the HFIW process. However, a comprehensive study is very difficult due to the multiple parameters that affect this process. Experimental and analytical studies show that the frequency, current, geometry of the contracted vee shape, and width of the sheet have the most significant effect on the HFIW process quality [2].

Saito et al. [3] presented an analytical model of heat distribution in the weld metal in HFIW process. They found that the highest concentration of heat occurs in the upper and lower edges of the sheets. The numerical model of the heat distribution is investigated by Inge and Grande [4]. Some studies have also examined the weld seam suitable for extra-low-temperature services [5]. In these studies, the temperature profile of the weld zone is determined. The formation mechanism of the internal and external beads has also been investigated [6]. The results of this study showed that the size of the bead increases due to an unnecessary increase in the energy input. The quality of the HFIW process has been investigated through photographing [7]. The results showed that the most important parameters involved in the welding quality are vee angle, welding speed, welding energy, compressive force, and weld frequency. The heated edges of the joint determine the density of the weld defects. Some of the HFIW process parameters such as vee angle and its effect on the temperature distribution in the weld metal have been investigated in [8]. The numerical analysis of the HFIW process [9] indicates that the edge preparation is a suitable way to prevent cold-welding and melting defects in the HFIW process. The appropriate edge shape reduces the temperature gradient at the edges of the sheet at the welding stage. On the inner and outer connecting edge, due to the skin and proximity effects, a very high thermal concentration occurs. The joint type decentralized the heat at these points. On the other hand, in appropriate edge shape, it causes metallurgical corrosion at the upper and lower edges of the pipe. This is due to the high temperature of the two surfaces relative to the center of the weld section.

HFIW process is a commonly used process in welded pipe manufacturing. The proper capabilities of this welding method are:

- Does not require any welding filler
- Welding quality does not depend on the welder's skill
- Easy automatic functionality in the high-speed linear products

Many researchers have studied this welding method. Reaching a uniform temperature distribution in the weld metal is vital. In the HFIW process, due to the skin and proximity effects, the heat concentrates on the upper and lower edges of the sheet. Chamfering the upper and lower edges of the sheets can prevent concentration of the heat at these edges. In other words, the joint type is very important. A proper weld profile will be obtained, if a roughly rectangular weld profile is formed. As a result, the joint will have high mechanical and metallurgical properties.

Thus, the main purpose of this paper is to investigate the effect of joint type on the temperature distribution and shape of the weld profile. So far, this research has been concentrated on reducing the welding gradient's temperature by changes in the welding parameters. Continuous products, such as welded pipes, have adjustable welding parameters and it is costly to change these parameters. Changing the joint type has the lowest cost in the product line. On the other hand, in order to achieve to a rectangular-shaped weld profile in the welded pipe, the joint type is the most important parameter [10, 11]. Concentrating on the effect of the joint type on the shape of the weld profile can be useful, and this could be the innovation of this paper. In this paper, to perform the welding process, a roll forming line with 8 stations and a high-frequency welding machine with a maximum output power of 300 kW were used. After welding, specimens were wire cut from the pipes and prepared for mechanical and microstructure examination.

2 Experimental procedure

The important factors affecting the HFIW process such as frequency, current, and shape of the joining edges in the seam-welded pipes have been experimentally studied according to API Specification 5L standard. L 210 carbon steel sheets with a thickness of 5 mm, as a commonly used material

Table 1 Chemical composition of L 210 carbon steel used in the experimental study

Fe	%C	%S	%P	%Mn	Other
base	0.22	0.03	0.03	0.9	Nb + V max 0.06

in the oil, gas, and petrochemicals industries, were used in this study. The chemical composition of this kind of carbon steel is presented in Table 1. Tensile strength and UTS of this sheet are reported as 340 and 446 MPa, respectively [12].

In order to perform experimental tests, three pieces of L210 steel sheet with a thickness of 5 mm and a width of 526 mm were used. For each piece, the edge geometry obtained from simulated data was applied on the experimental specimens.

Based on the thickness and diameter of the pipe, the power of 144 kW was used for induction welding. Since induction welding is an automatic process and there are no human errors, the vee-shaped zone in the sheet edges is the only variable in the experimental tests. Three kinds of edge geometry, specimens A, B, and C, were used according to the forthcoming numerical simulations, as shown in Fig. 2.

All the specimens were welded using HFIW process and primary quality controls were performed to ensure all are defect-free.

The following parameters were considered in the HFIW process:

- Distance between the inductor center and weld zone was 22 cm.
- The distance between the edges at the beginning of inductor was 14 mm.
- The vee angle was 2.5°.

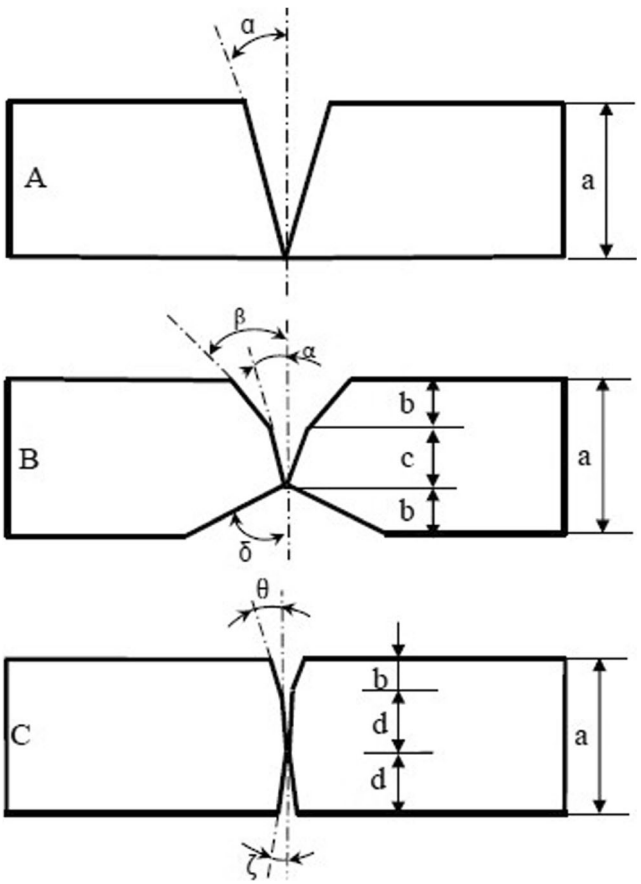

Fig. 2 Schematic of edge preparing in the experimental tests. $a = 5$ mm, $b = 1.5$ mm, $c = 2$ mm, $d = 1.75$ mm, $\alpha = 6°$, $\beta = 24°$, $\delta = 53°$, $\theta = 14°$, and $\zeta = 10°$

Figure 3 shows the experimental system of HFIW process used in these experiments. As shown in Fig. 3, coolant fluid is used in the process of welded pipe production by HFIW method. It is compulsory to use this coolant fluid due the high temperature around the weld metal. The coolant fluid prevents some defects, such as creation of super-melting temperature in the weld metal. So, manufacturers should use this coolant. There is no way to measure the temperature of the weld metal by tools such as thermography. The temperature contours make the final weld shape and the simulation can be verified, and this is the only possible way.

3 Modeling of HFIW process

3.1 Theoretical aspect

To calculate the induced current in the circular coils, the cushy static equations need to be solved to get the static magnetic potential [13]:

$$\sigma\frac{\partial \boldsymbol{A}^{*}}{\partial t}+\nabla\times\left(\frac{1}{\mu_0\mu_{\mathrm{r}}}\nabla\times\boldsymbol{A}^{*}\right)=\sigma\frac{Nl_{\mathrm{coil}}}{A}e_{\mathrm{coil}} \tag{1}$$

where A is the cross-section of inductor (m^2), A^* is the magnetic potential (Wb/m), l_{coil} is the length of a round coil (m), σ is the electrical conductivity (S/m), μ_0 is the magnetic permeability of vacuum, μ_r is the permeability of inductor, and N is the number of inductor rounds. Equation 1 shows that the pipe schedule, the length of the vee-shaped area, and the standard penetration depth and form are the most important geometric parameters affecting this process. Due to the skin effect, the electrical current passes superficially at high frequencies, making the current penetrate lower depths of the conductor.

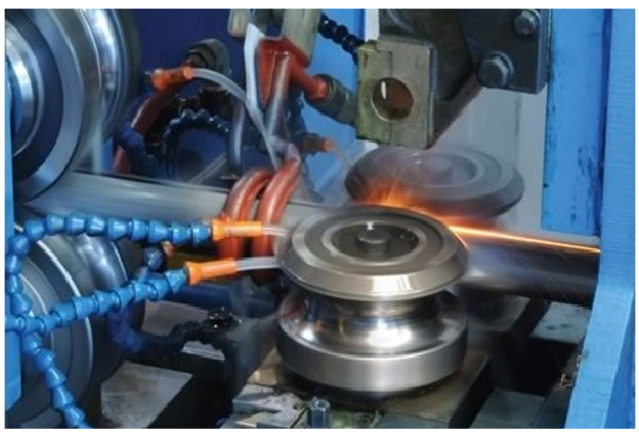

Fig. 3 High-frequency induction welding system used in the experiments

The standard penetration depth is obtained from the following equation [14]:

$$\delta = \sqrt{\frac{1}{\pi f \mu \sigma}} \tag{2}$$

where μ is the magnetic permeability (H/m), σ is the electrical conductivity (1/Ω.m), and f is the frequency of the current (Hz).

3.2 Numerical analysis

A finite element model is used to study the temperature distribution in the weld zone of the seam-welded samples. The principle of conservation of energy (Bayot-February equation) is used in the numerical modeling of heat generation during HFIW process.

The model used in the numerical analysis in this paper is based on other related research [11, 15, 16]. Using these equations defines the boundary conditions in COMSOL software. In this paper, the boundary conditions are considered in accordance with the experimental conditions. Some boundary conditions are explained in relations 3–6 and others are considered as follows.

The pipe considered in the FE model has a diameter of 165.2 mm, wall thickness of 5 mm, and length of 1000 mm. Parameters such as current, frequency, and traveling speed, considered constant, are equal to 1400 A, 150 kHz, and 25 m/min respectively. Electrical, thermal, and magnetic properties of the material have been imported to the FE model as a function of temperature.

By inducing the electrical current to the model, internal resistance heats the edges of the simulated model up to the welding temperature. The heat generated in the pipes is created based on the subsequent equations [17]. Assuming that all of the input power is converted into the surface heat, the average heat input can be calculated using the following equations:

$$\rho C_{\mathrm{p}} u.\nabla T = \nabla.(k\nabla T) + Q_e \tag{3}$$

$$Q_e = Q_{\mathrm{rh}} + Q_{\mathrm{ml}} \tag{4}$$

$$Q_{rh} = \frac{1}{2} R_{\mathrm{e}}(J.E) \tag{5}$$

$$Q_{ml} = \frac{1}{2} R_{\mathrm{e}}(iwB.H) \tag{6}$$

where Q_{rh} is the resistive loss (W/m^3), Q_{ml} is the magnetic loss (W/m^3), C_{p} is the heat capacity (J/kg/K), ρ is density (kg/m^3), and u is linear speed (m/s). The COMSOL finite element software is used to accomplish the required simulations and analyze the HFIW process. The modeling was carried out based on the experimental pipe geometry and fin pass station. The edges of the fin pass station have an angle of 5° relative to each other, before the welding station. Maxwell's equations have been used for the electrical and magnetic calculations in the COMSOL software, and the heat generated at the edges is achieved through converting electrical losses. It should be noted that Eq. 3 is extracted from the magnetic simulation physics section of the COMSOL software. In these simulations, phase change is not considered, and the metal is heated up to the melting point. If the melting point is reached or passed, the materials will be completely plastic. It should be noted that the pipe and coil type in this simulation are steel and copper, respectively. Tables 2 and 3 show the material properties of the pipe and coil in this simulation.

The value of these parameters is determined by the experimental results of pipe manufacturers. Two charts of Figs. 5 and 6 have been used to determine the changes in material properties due to temperature in these simulations.

3.3 Parameters of HFIW

Induction welding process includes electrical, magnetic, thermal, and mechanical modules [18]. The numerical analysis of this process is very complex due to the multi-field and transient nature of the process. To simulate the energy input to the process, four media are used in different fields mentioned. Carbon steel was used as the pipe material. The angle of 2.5° has been considered in the vee- and Y-shaped zones. A three-dimensional 4-node and 4-face tetrahedral mesh is used in modeling, which includes the magnetic and temperature degrees of freedom. The experimental and simulation results were compared to ensure the accuracy of modeling.

Figure 4 represents the created model in the software. Temperature-dependent material properties used in this simulation are shown in Figs. 5 and 6.

The geometry of the welding edges of the pipe is obtained according to the shape of the blades in the fin pass station. Then, by performing simulations and modifying the edge geometries to the better ones, an improved shape has been

Table 2 Material properties intended for the welded pipe in the simulation

Property	Value	Unit
Relative permeability	100	1
Electrical conductivity	4.032E6	s/m
Relative permittivity	1	1
Thermal conductivity	44.5	W/(m K)
Density	7850	kg/m^3
Heat capacity at constant pressure	475	J/(kg K)
Young's modulus	206	GPa
Poisson's ratio	0.29	1
Initial yield stress	450	MPa

Table 3 Material properties intended for the coils in the simulation

Property	Value	Unit
Relative permeability	1	1
Electrical conductivity	5.998e7	S/m
Coefficient of thermal expansion	17e−6	1/K
Heat capacity at constant pressure	385	J/(kg K)
Relative permittivity	1	1
Density	8960	kg/m^3
Thermal conductivity	400	W/(m K)
Young's modulus	110e9	Pa
Poisson's ratio	0.35	1
Reference resistivity	1.72e−8	Ω m
Resistivity temperature coefficient	0.0039	1/K

proposed for connecting edges in the welding station. To achieve the lowest temperature gradient in the welded edges, several simulations with different edges have been made and this process is carried out sequentially.

3.4 Investigation of effects of the edge geometry

Different simulations were made with edge preparation of the sheet to reduce the temperature gradient in the weld zone and achieve the optimal edge shape with the lowest temperature gradient. The first simulation with an unprepared edge resulted in the highest temperature gradient at the weld zone, where the skin and proximity effects obviously increase the temperature of the inner part of the welding edge more severely.

To approach the melting point in every part of the edge, more electrical current should be induced, leading to more power consumption, and thereby energy costs increase. On the other hand, increasing the temperature of the whole edge to the minimum welding temperature will also increase the temperature in the inner part of the edges. So, when the outer edge reaches the minimum temperatures of joining, the inner edge will be overheated to the melting temperature, making internal edges overmelted and, thus, burning occurs. Moreover, applying more power to reach the joining temperature increases the weld width and expands the heat-affected zone.

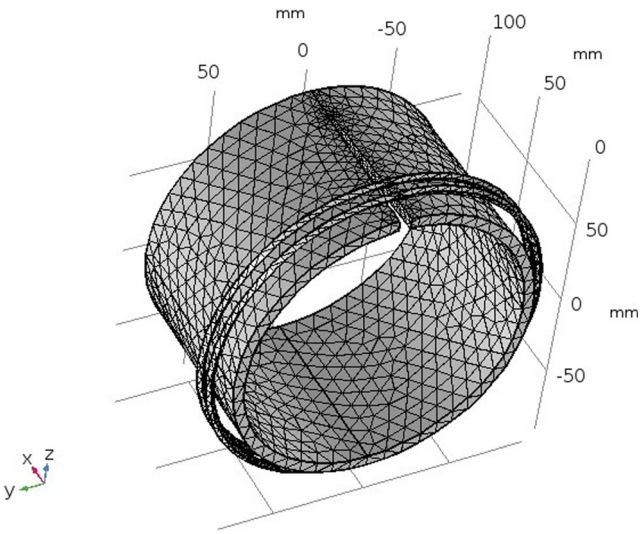

Fig. 4 Finite element model meshed with tetrahedral elements

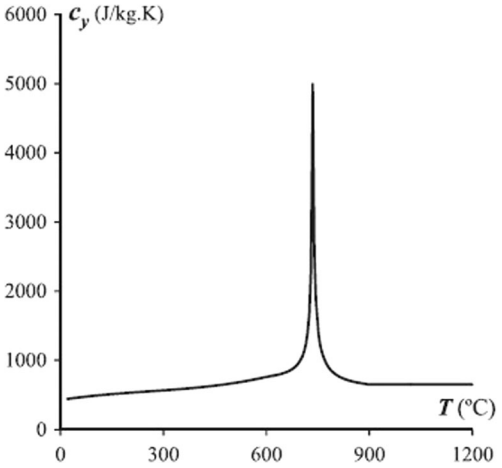

Fig. 5 Specific heat at different temperatures for structural steel [14]

Modifying the shape of the edges can beneficially decrease the temperature gradient to reach uniformity along the whole edge of the weld. After trying some edge geometries, the final modified edge shape can be used to carry out the experimental tests.

Temperature changes in four zones of the join edge according to the simulation of sample A and away from the center line of the weld are shown in Fig. 7.

As shown in Fig. 7, temperature gradient of about 1200 °C is created at the first edge. Based on iso-thermal diagrams obtained from the simulations, the geometry of the weld edge was modified and used in modeling. The final goal of modifying joint types was making an edge with a minimum temperature gradient. Improved edge shapes are obtained in the

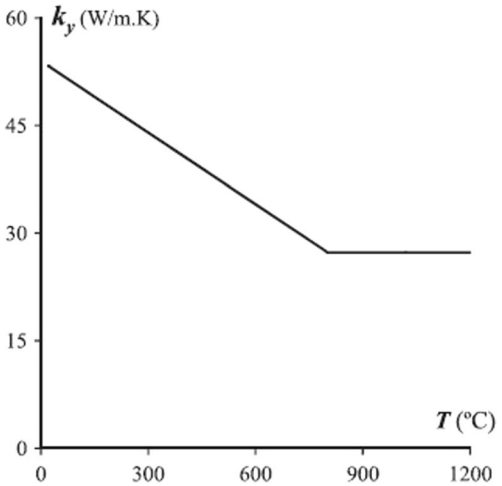

Fig. 6 Thermal conductivity at various temperatures for structural steel [14]

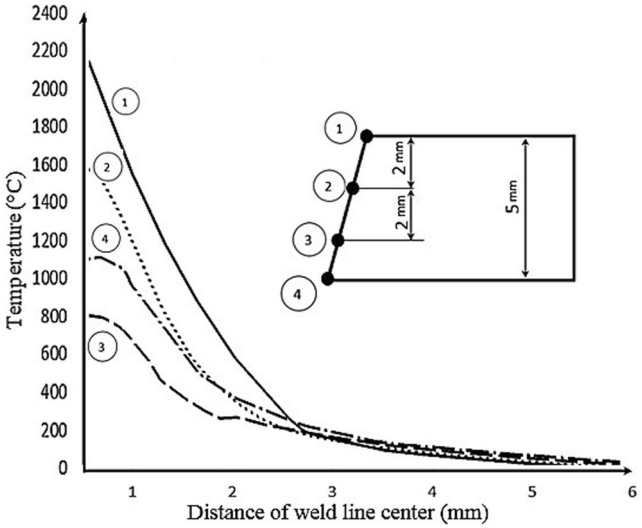

Fig. 7 Maximum temperature of 4 zones in the weld edge of sample A

forms shown in Fig. 2 (samples B and C). Numerical analysis of three prepared edge samples of Fig. 2 shows that the edge geometry is an important parameter affecting the temperature gradient of the welded pipe. According to the results, final edge shape (Fig. 2(C)) has the lowest temperature gradient and, thus, the temperature distribution is monotonous. The temperature distributions at the edges are shown in Figs. 8 and 9, in two power sets of 123 kW (a) and 179 kW (b) and in two different edge geometries B and C. In these figures, the temperature gradients are shown as iso-thermal lines in the prepared edge shapes.

As the images of the temperature contours show, the temperature concentration at the lower edge is higher than the upper edge. This temperature concentration difference is due to the presence of impeder inside the welded pipe. The impeder increases the proximity properties; hence, the concentration of heat at the lower edge is higher.

By performing these simulations, the improved edge geometry connecting to the welding stations has been proposed. Figure 9 shows the temperature distribution at the edges of sample C as the final improved edge geometry.

Increasing the welding power leads to an increase in the weld profile width and the heat-affected zones. By comparison, the power consumption of welding in sample B is 30% higher than that of modified edge of sample C. Moreover, in heating sample B, the whole edge does not reach the minimum welding temperature at once. This leads to a 60% increase in the total energy consumption. Temperature distribution in four locations of the joint edge in sample C is shown in Fig. 10.

Comparing Figs. 7 and 10 shows that the temperature gradient is decreased from 1200 to 200°. This reflects the strong effect of the edge shape preparation on the uniformity of temperature distribution at the edge of the joint. Heating process in the vee-shaped and weld zones is important: the greater the weld zone, the higher the heat losses. On the other hand, if the

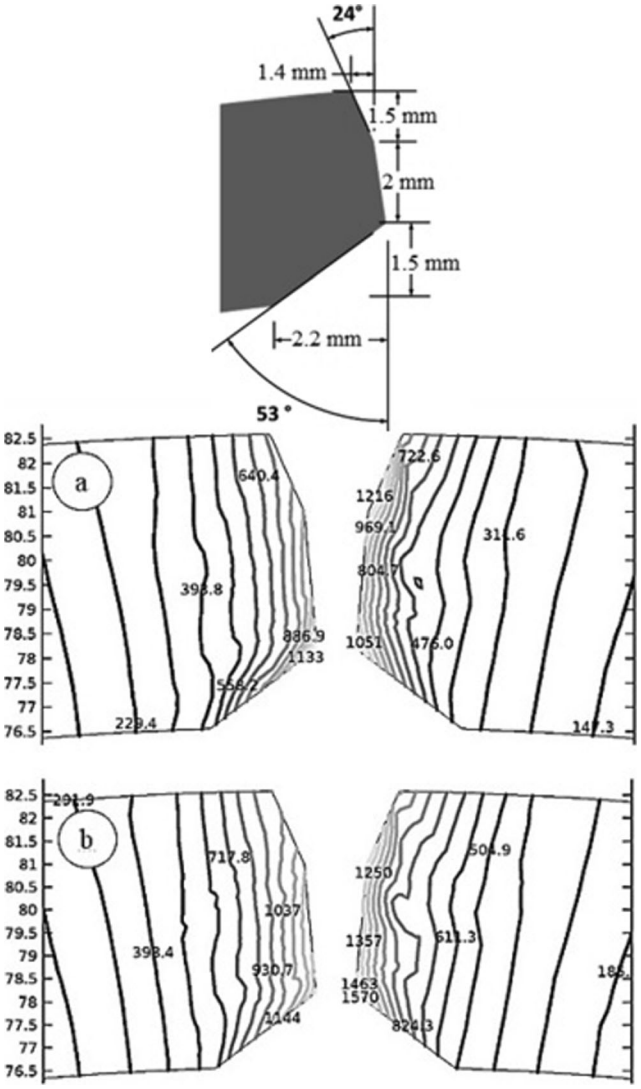

Fig. 8 Temperature distribution as iso-thermal lines in the sample B for two power sets

generated temperature during welding is lower than the optimal limit, it shows that mixing is weak and the welded specimen does not meet the adequate strength. For this reason and due to the effect of the welding parameters on heat generation during the welding process, microstructures of the heat-affected and thermomechanical zones have been investigated and compared in the two abovementioned samples.

In Fig. 11, the weld profile without a joint type and specimens A, B, and C are shown. Specimen C has the lowest weld width and specimen W has the widest weld width.The rectangularity of the weld profile in A, B, and C specimens indicates the importance of the joint type and validates the simulations and temperature contour.

Comparing Fig. 11 and Figs. 8 and 9 shows that simulation and experimental results are consistent with each other. In specimen C in Fig. 11 there is no rectangular weld section. This curvature in the sidewall of the weld metal indicates the

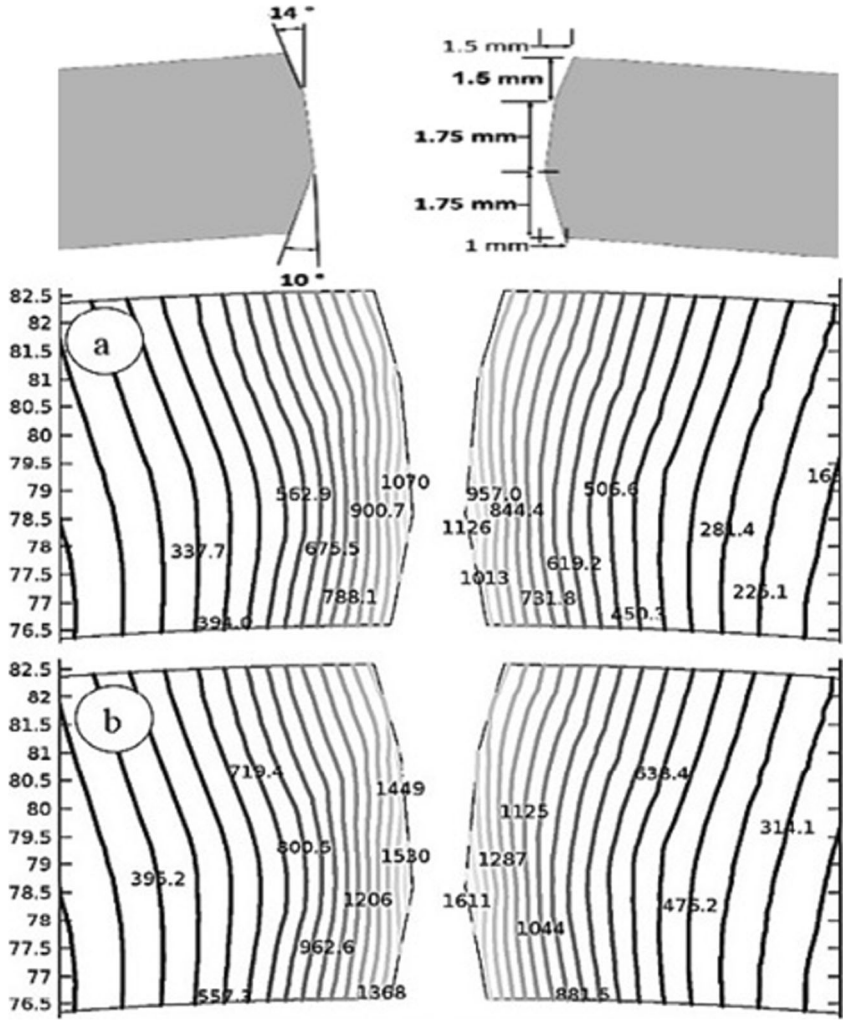

Fig. 9 Temperature distribution as iso-thermal lines in the sample C in two power sets

higher input temperature at the upper and lower edges of the sheet. The skin and proximity effects on the HFIW process cause the upper and lower edges of the sheet to undergo more heat than the center. Chamfering the upper and lower edges of the sheet can be a good way to prevent overheating of the edges. In other words, selecting a proper joint type can decrease the effects of the high-frequency current (skin and proximity effects) on the edges overheating. So, the edges do not suffer excessive heat. The uniform temperature created at the edges of the weld line because of the joint type leads to a joint with high mechanical and metallurgical properties.

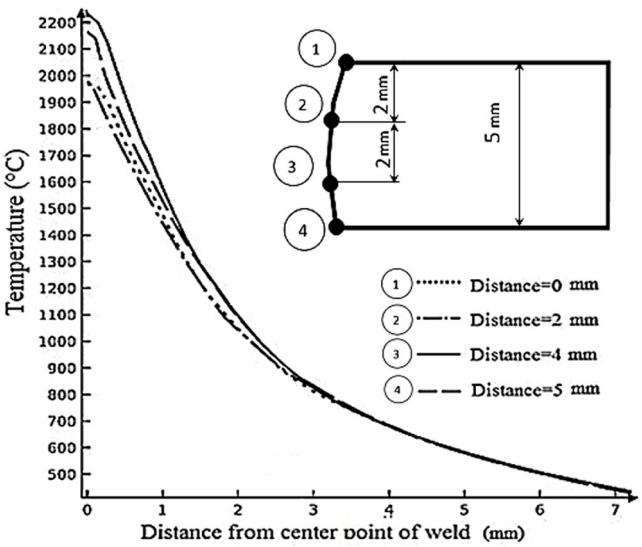

Fig. 10 Temperature distribution in 4 different locations in sample C

4 Results and discussion

4.1 Tensile test

To reach the expected mechanical properties in the welded joints, tensile tests according to the ASTM-E8 standard [19] were used. Test specimens were prepared using wire cut from the experimental test pipes as shown in Fig. 12. To ensure the repeatability of the test results, from each case study, three

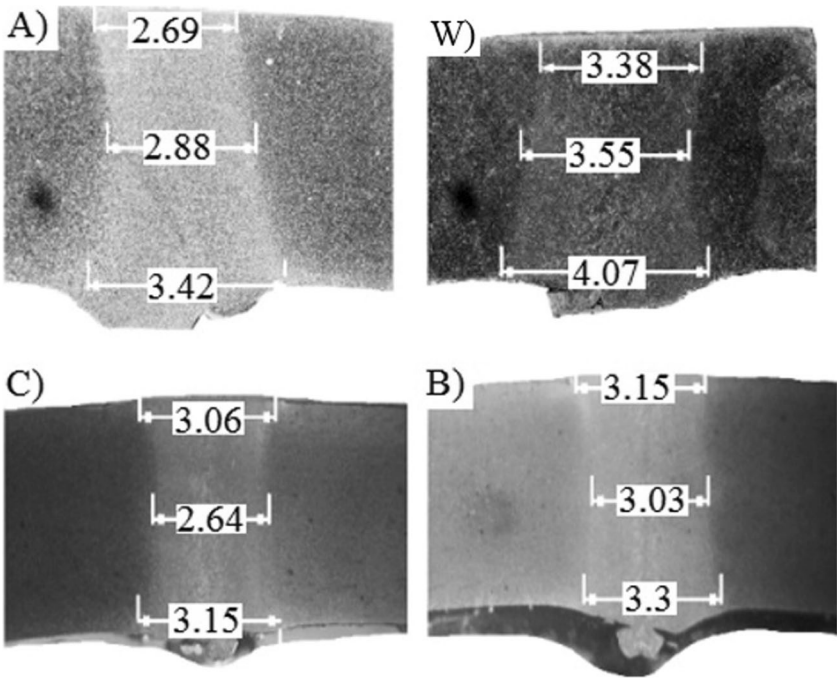

Fig. 11 Uniformity comparison of weld's width in several edge shapes (W) without edge preparing, (A) specimen A, (B) specimen B, and (C) specimen C

specimens were prepared and tested. According to Fig. 12, specimen D refers to the tensile test of the base metal sheets.

Figure 13 shows the column graphs of the ultimate and yield tensile strength in specimens A, B, and C.

In Fig. 14, the elongations of these specimens are compared. The observed trend in the yield strength shows that improving the shape of the edge increases the tensile strength to some extent. The average increase in the strength of the improved specimens is 5.7%. The rapture area in the specimens is distant from the weld line, indicating weld health. Also, the maximum elongation of specimen C was increased from 17.5 to 19.1%, compared with the specimens without edge preparation (specimen A). The increase in the mechanical properties results can be derived from the uniformity of the weld zone and, consequently, the reduction of weld defects.

4.2 Macro- and microstructure

Due to the interaction of thermal and mechanical mechanisms in HFIW process, four metallurgical regions can be specified [20]. These four regions are shown in Fig. 15. At the bottom of this image, micrographic images are shown in four different weld zones: base metal (BM), heat-affected zones (HAZ), thermomechanical affected zone (TMAZ), and the fusion zone (FZ). In this figure, the different regions of the weld profile, which will be described below, are marked and separated by lines.

Metallography of the welded specimens in three joint types represents different structures in this region, including coaxial ferrite grains and perlite boundaries.

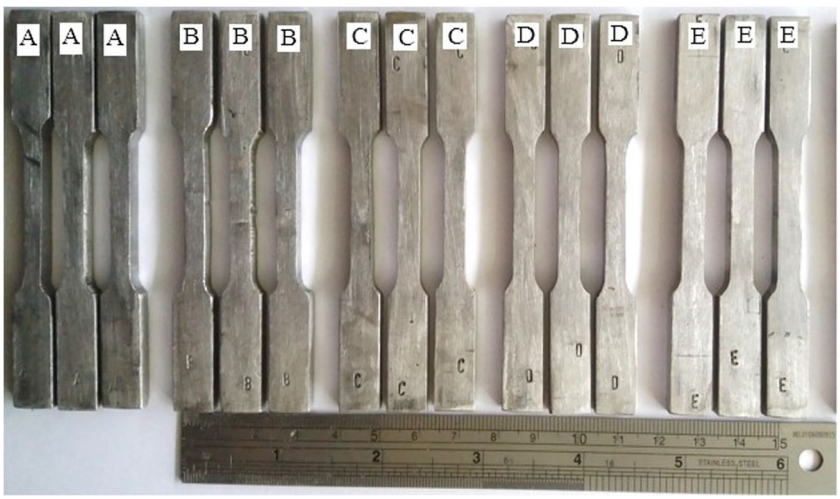

Fig. 12 Tensile test specimens based on ASTM-E8 (subsize) standard for large diameter HFI-welded pipes

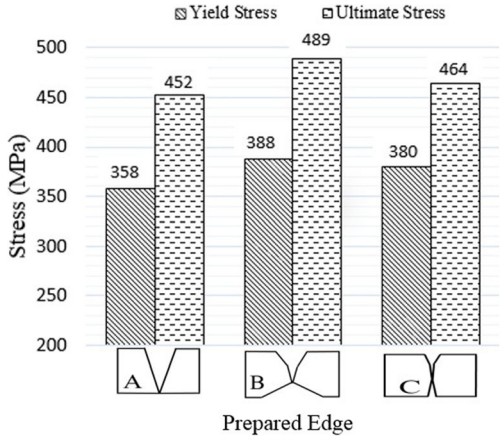

Fig. 13 Yield and ultimate strength of the welds in the different edge preparations

They also indicate differences in the grain size in the base metal, weld heat-affected zones, and the thermomechanical zone. Metallographic investigations on the specimens in more instances show the following for microstructure areas:

Base metal zone has regular ferrite grains, fine and normalized, with boundaries of pearlite. The average grain size in this region is about 7.6 μm. In the case of grain alignment in the direct formation of ferrite, the probability of crack formation and growth is high, but no crack was seen in the thermomechanical region.

Heat-affected zone has finer grains compared with the two previous zones. The average grain size is measured as 5.7 μm. The HAZ has a fine grain microstructure of ferrite, with pearlite buds grown in the ferrite base.

Thermomechanical zone is a zone with coaxial grains through the protrusions of the weld metal area. Grain size in this zone is almost equal to the base metal, but in terms of direction, these two zones differ from one another. The microstructure of the thermomechanical zone is similar to the base metal, but the ferrite grains are not identical. This zone appears only at the top and bottom of the welded joints and cannot be clearly seen in the center.

Fusion zone is the closest zone to the weld center. This zone is melted by heat. After the pressure of the welding rollers, this area becomes solid. The fusion zone reaches temperatures higher than the austenitic temperature and undergoes rapid cooling; thus, it has fine and irregular grains. The average grain size in this region is about 5.6 μm.

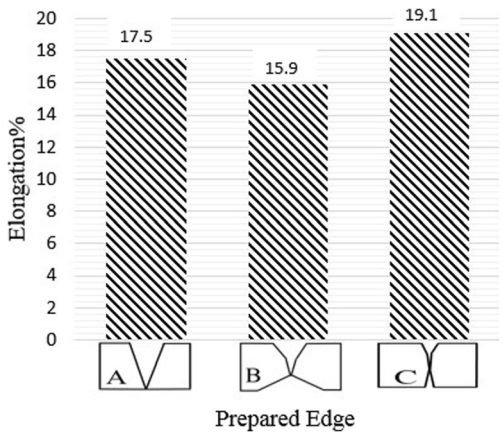

Fig. 14 Comparison of the elongation in three specimens A, B, and C

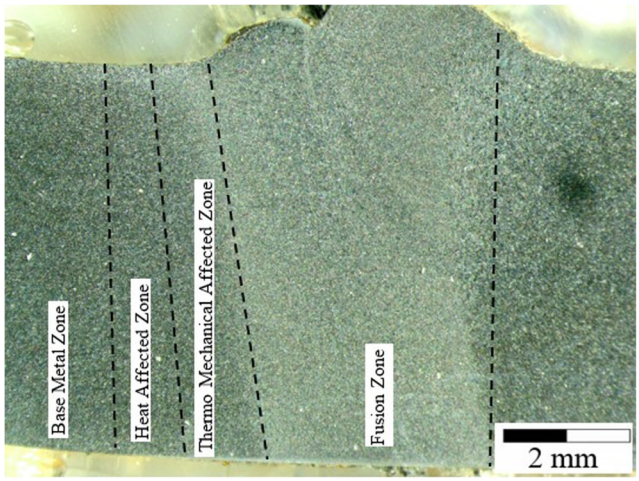

Fig. 15 Cross-section of the weld and 4 difference zones. Base metal (BM), heat-affected zone (HAZ), thermomechanical affected zone (TMAZ), and fusion zone (FZ)

4.3 Weld zone uniformity

The weld width in the specimens without edge preparation is greater in the inner weld part than that of the outer part, whereas in the properly beveled specimens, the upper and lower parts are of the same width. In average, in specimens without edge preparation, the weld width along the heat-affected zone in the internal weld area is about 1.5 times the outer area. The resulting weld area in the improved specimens has a more uniform width in the center, top, and bottom of the weld. However, as it can be seen, in the inner parts of the experimental specimens, the weld width is greater than the outer part, representing more melting in the internal parts. The same trend is observed in the simulation results. Figure 16 shows the comparison of experimental and simulation results to calculate the welding width of specimen C. In Fig. 17, the experimental and simulation results of the width of the weld area in the three specimens at 5 distances from outer surface of the weld edge are compared. By improving the shape of the edges, the weld width is reduced and its uniformity across the thickness is improved. Both phenomena have a positive effect on the quality of the HFI welds.

The difference in the simulation and experimental results can be attributed to the environmental conditions in the

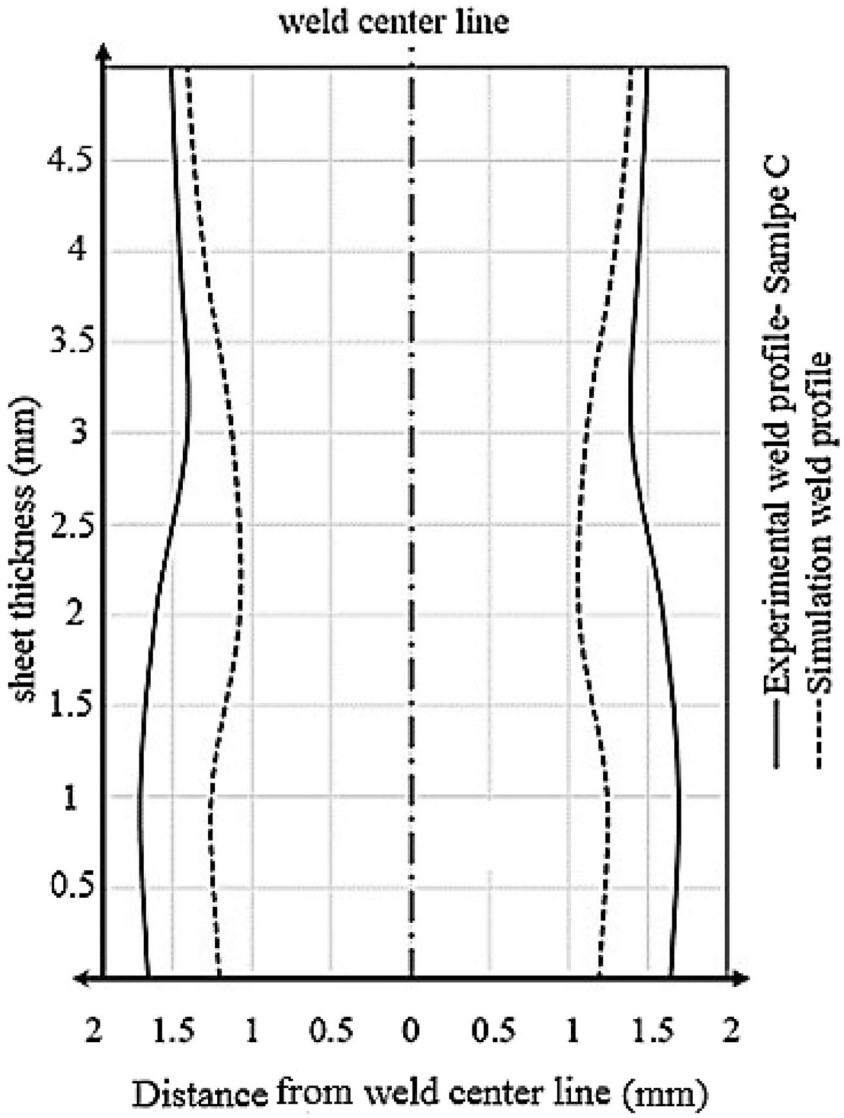

Fig. 16 Comparison of experimental and simulated weld width and profile on the specimen C

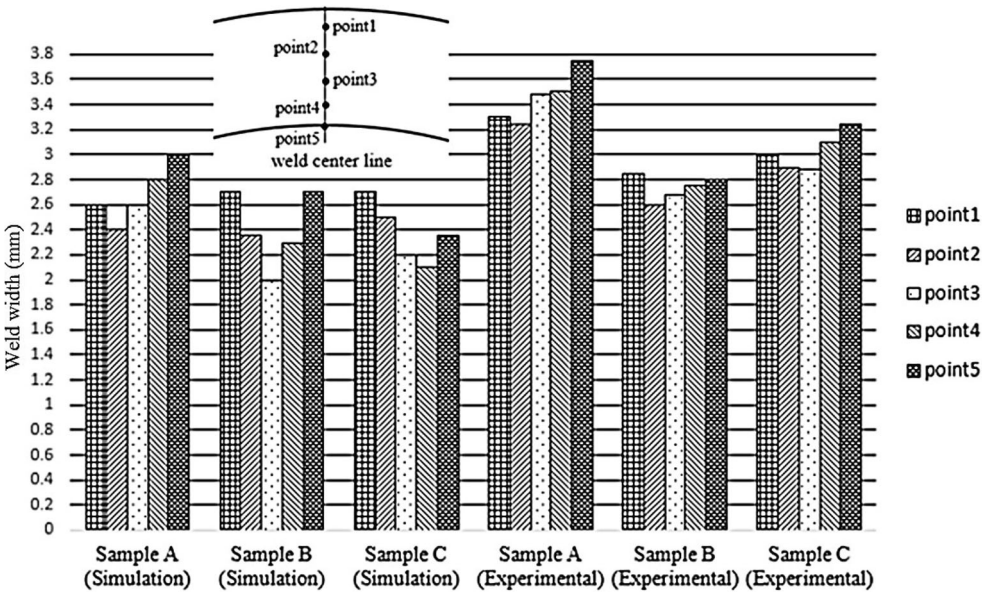

Fig. 17 Comparison of weld width in different points of three specimens' experimental and simulation results

empirical tests. For example, in a high-frequency current transmission circuit, the resistance created in environmental conditions will be greater than the ideal condition in the simulations. Some environmental conditions that increase electrical resistance include the following: surface contamination of the edge due to the application of cooling fluids, the presence of impurities in the sheet, the surface finish oxidation, and the surface flatness of the edges. Hence, the simulation predicts a weld width slightly less than experimental values. In addition, the weld width is measured using cross-sectional metallography in a practical test, in which some of the measurement errors may also affect the responses.

In the second edge shape, heat distribution is not uniform at the edges during the process, so the material flow is improper. Weld bead shape at these specimens shows a little stir action of the edges. In specimens with final edge shape (C), heat distribution across the entire edge line is uniform. Thus, edge stirring action and material flow are more proper, decreasing the weld width. The stirring action of edges is increased in the final modified specimens.

5 Conclusion

In this paper, HFIW process and the effect of different process parameters on improving the weld quality of pipes were studied. The most important parameter affecting the quality of the HFIW process is the temperature gradient at the connecting edges. Reducing the temperature gradient or, in other words, uniformity of the temperature distribution at the edge of joint will improve the process and increase the quality of the weld zone.

The results show that improving the geometry of the welding edge reduces the temperature gradient at the surface of the joint. In one case, the temperature gradient decreased about 600 °C with just edge modification. The reason is the reduction of the heat transfer in cross-section and the uniformity of the thermal flux along the edges as well as vee-shaped region. Therefore, it can be concluded that for controlling the temperature gradient at the edges, improving the edge shape of the unshaped sheets is a cost-effective and efficient method.

Investigation of different microstructures in the weld area shows a reduction in the size of the grains in the weld metal, the heat-affected zone, and the thermomechanical regions. By modifying the edge shape, greater reduction in the grain size occurred in the weld metal, which was estimated about 27%. Also, the decrease in the mean grain size in the heat-affected and thermomechanical regions was 18.5 and 17%, respectively.

Simulations that were carried out at weld metal without joint type show an increase in the proximity effect, which eventually increases the temperature of the edges. The simulation results also show that the highest temperature rise occurs in the specimens in which the upper and lower edges of the sheet are not chamfered (without joint type). Reducing the temperature gradient by employing an improved edge shape in the HFIW process improves mechanical and metallurgical properties and, at the same time, reduces the power consumption in the process.

References

1. Okabe T, Yasuda K, Nakata K (2014) Dynamic observations of welding phenomena and finite element analysis in high frequency electric resistance welding. Quarterly Journal of The Japan Welding Society 32(3):156–163
2. Okabe T, Iizuka Y, Igi S (2014) High reliability technology of the weld zone of high-frequency electric resistance welding linepipes. JFE Technical Report 34:77–83
3. Saito M, Kasahara H, Tominaga H, Watanabe S (1986) Theoretical analysis of current distribution in electric resistance welding. Transactions of the Iron and Steel Institute of Japan 26(5):461–467
4. Nikanorov A, Baake E, Neumeyer J (2015) Numerical simulation and investigation of high frequency tube welding process. Appl Mech Mater 698:245–250
5. Shunsuke T, Sota G, Takatoshi O, Hideto K, Satoshi L (2015) Metallurgical design and performance of high-frequency electric resistance welded linepipe with high-quality weld seam suitable for extra-low-temperature services. Journal of Offshore Mechanics and Arctic Engineering 137:1–11
6. choi J, chang Y, kim C, OH J, kim Y (2004) Penetrator formation mechanisms during high-frequency electric resistance welding. Weld J 27–31
7. Kim T, Park Y, Sung K, Kang M, Kim C, lee C et al (2007) Estimation of weld quality in high-frequency electric resistance welding with image processing. Weld J 7:1–9
8. Kim H-J, Youn S-K (2008) Three dimensional analysis of high frequency induction welding of steel pipes with impeder. J Manuf Sci Eng 130(3):031005–031007
9. han Y, yu E (2012) Numerical analysis of a high-frequency induction welded pipe. Weld J :270–7
10. Choong-Myeong K, Jung-Kyu K (2009) The effect of electromagnetic forces on the penetrator formation during high-frequency electric resistance welding. J Mater Process Technol 209:838–846
11. Sung-Soo E, Min-Hyun C, Ki-Hong K, Hyun-Seung L (2012) Development of optimum welding heat input device based on welding frequency and spark detection. Proceedings of the 2012 9th international pipeline conference: 24–28
12. Forzan M, Garbin M, Dughiero F, Sieni E, Pozza C (2011) A 3D numerical FEM model for the simulation of induction welding of tubes. COMPEL - The international journal for computation and mathematics in electrical and electronic engineering 30(5):1570–1581
13. Baumer R, Adonyi Y (2009) Transient high-frequency welding simulations of dual-phase steels 88: 193–201
14. Kasaei MM, Moslemi Naeini H, Azizi Tafti R, Tehrani MS (2014) Prediction of maximum initial strip width in the cage roll forming process of ERW pipes using edge buckling criterion. J Mater Process Technol 214(2):190–199
15. Santana IJ, Paulo B, Modenesi PJ (2006) High frequency induction welding simulating on ferritic stainless steels. J Mater Process Technol 179:225–230
16. Yu EL, Han Y, Fan Y, Zhao Y (2010) Simulation of coupling of electromagnetic and thermal fields for process of high-frequency

induction heating of HFW pipe. Hanjie Xuebao/Transactions of the China Welding Institution 31:5–8

17. Choong K, Jung-Kyu K (2009) The effect of heat input on the defect phases in high frequency electric resistance welding. Met Mater 1:141–148
18. Udhayakumar T, Mani E (2017) Effect of HF welding process parameters and post heat treatment in the development of micro alloyed HSLA steel tubes for torsional application. J Mater Sci Eng 6:1–8
19. Standard Test Methods for Tension Testing of Metallic Materials (2007) ASTM Standard
20. Yan P, Gungor OE, Thibaux P, Liebeherr M, Bhadeshia HKDH (2011) Tackling the toughness of steel pipes produced by high frequency induction welding and heat-treatment. Mater Sci Eng A 528(29):8492–8499

Publisher's note Springer Nature remains neutral with regard to jurisdictional claims in published maps and institutional affiliations.